



Published in final edited form as:

Nature. 2013 August 1; 500(7460): 93–97. doi:10.1038/nature12287.

A stable transcription factor complex nucleated by oligomeric AML1-ETO controls leukaemogenesis

Xiao-Jian Sun¹, Zhanxin Wang², Lan Wang^{3,4}, Yanwen Jiang⁵, Nils Kost⁶, T. David Soong⁷, Wei-Yi Chen¹, Zhanyun Tang¹, Tomoyoshi Nakadai¹, Olivier Elemento⁷, Wolfgang Fischle⁶, Ari Melnick⁵, Dinshaw J. Patel², Stephen D. Nimer^{3,4}, and Robert G. Roeder¹

¹Laboratory of Biochemistry and Molecular Biology, The Rockefeller University, New York, New York 10065, USA

²Structural Biology Program, Sloan-Kettering Institute, Memorial Sloan-Kettering Cancer Center, New York, New York 10065, USA

³Molecular Pharmacology and Chemistry Program, Sloan-Kettering Institute, Memorial Sloan-Kettering Cancer Center, New York, New York 10065, USA

⁴Sylvester Comprehensive Cancer Center, Miller School of Medicine, University of Miami, Miami, FL 33136, USA

⁵Division of Hematology and Medical Oncology, Department of Medicine, Weill Cornell Medical College, New York, New York 10065, USA

⁶Laboratory of Chromatin Biochemistry, Max Planck Institute for Biophysical Chemistry, 37077 Göttingen, Germany

⁷Institute for Computational Biomedicine, Weill Cornell Medical College, New York, New York 10065, USA

Abstract

Transcription factors are frequently altered in leukaemia through chromosomal translocation, mutation or aberrant expression¹. AML1-ETO, a fusion protein generated by the t(8;21) translocation in acute myeloid leukaemia (AML), is a transcription factor implicated in both gene repression and activation². AML1-ETO oligomerization, mediated by the NHR2 domain, is critical for leukaemogenesis^{3–6}, making it important to identify coregulatory factors that “read”

Users may view, print, copy, download and text and data- mine the content in such documents, for the purposes of academic research, subject always to the full Conditions of use: http://www.nature.com/authors/editorial_policies/license.html#terms

Correspondence and requests for materials should be addressed to R.G.R. (roeder@rockefeller.edu).

Supplementary Information is linked to the online version of the paper at www.nature.com/nature.

Author Contributions X.J.S. and R.G.R. conceived the project. R.G.R. supervised the biochemical studies. S.D.N. supervised the leukaemia pathological studies. D.J.P. supervised the structural studies. A.M. supervised the genomic studies. X.J.S., Z.W., L.W., Y.J., N.K., T.D.S., W.Y.C., Z.T., T.N., O.E. and W.F. performed the experiments and analyzed the data. X.J.S. and R.G.R. wrote the paper.

ChIP-seq and RNA-seq data have been deposited in GEO under accession number GSE43834. Crystal structure of the NHR2-N2B complex has been deposited in PDB under accession code 4JOL.

Reprints and permissions information is available at www.nature.com/reprints.

The authors declare no competing financial interests.

the NHR2 oligomerization and contribute to leukaemogenesis⁴. We now show that, in leukaemic cells, AML1-ETO resides in and functions through a stable protein complex (AETFC) that contains several haematopoietic transcription (co)factors. These AETFC components stabilize the complex through multivalent interactions, provide multiple DNA-binding domains for diverse target genes, colocalize genome-wide, cooperatively regulate gene expression, and contribute to leukaemogenesis. Within the AETFC complex, AML1-ETO oligomerization is required for a specific interaction between the oligomerized NHR2 domain and a novel NHR2-binding (N2B) motif in E proteins. Crystallographic analysis of the NHR2-N2B complex reveals a unique interaction pattern in which an N2B peptide makes direct contact with side chains of two NHR2 domains as a dimer, providing a novel model of how dimeric/oligomeric transcription factors create a new protein-binding interface through dimerization/oligomerization. Intriguingly, disruption of this interaction by point mutations abrogates AML1-ETO-induced haematopoietic stem/progenitor cell self-renewal and leukaemogenesis. These results reveal new mechanisms of action of AML1-ETO and a potential therapeutic target in t(8;21)⁺ AML.

AML1-ETO consists of the DNA-binding (RUNT) domain of the haematopoietic transcription factor AML1/RUNX1 and four conserved domains (NHR1-4) of ETO². These domains differentially contribute to AML1-ETO activities in regulating cell proliferation, differentiation and survival². In particular, the NHR2-mediated oligomerization of AML1-ETO has been shown to be critical for leukaemogenesis³⁻⁶. While oligomerization endows AML1-ETO with a DNA-binding preference for duplicated AML1 sites⁷, it is important to explore the possibility that oligomerization might also affect cofactor recruitment and function. AML1-ETO is generally thought to act as a transcriptional repressor by recruiting corepressors (e.g., NCoR and HDACs) to AML1 target genes⁸⁻¹⁰ or by interacting and interfering with other transcription factors (e.g., ETS family proteins, C/EBP α , GATA1 and E proteins)¹¹⁻¹⁷. In relation to its functions in gene activation, AML1-ETO also can recruit coactivators p300¹⁸ and PRMT1¹⁹. Beyond these indications of dynamic AML1-ETO interactions with diverse proteins, it has been unclear whether AML1-ETO resides in any stable multiprotein complex(es) that might endow it with new properties that lead to altered regulatory events and corresponding cellular functions.

To identify a natural AML1-ETO-containing complex in leukaemic cells, we used patient-derived Kasumi-1 cells and an antigen-purified anti-ETO antibody that showed high specificity and affinity (Supplementary Fig. 2a, b). The absence of wild-type (WT) ETO in Kasumi-1 cells²⁰ allowed selective isolation of AML1-ETO from derived nuclear extracts, which contained most AML1-ETO (Supplementary Fig. 2c). Using a high stringency buffer to preclude weak or non-specific interactions, we isolated a stable AML1-ETO-containing transcription factor complex (AETFC) whose components were identified by SDS-PAGE (Fig. 1a) and mass spectrometry (Supplementary Fig. 3a) and confirmed by immunoblot (Fig. 1b). These components include the AML1-binding partner CBF β , E proteins HEB and E2A, the haematopoietic E-box-binding transcription factor LYL1 (but not its homologue SCL/TAL1), the LIM domain protein LMO2 and its interacting partner LDB1. While interactions among some of these factors (or homologues) have been implicated in a related GATA1-SCL-E2A-LMO2-LDB1 complex in erythrocytes²¹, their connection with AML1-ETO in AML is unknown. A gel-filtration analysis indicated that they form a stable, high

molecular weight complex (Supplementary Fig. 3b). We then employed baculovirus vectors to reconstitute AETFC and to characterize the pairwise interactions within AETFC (Supplementary Fig. 3c, d). The results revealed an interaction network (Fig. 1c) in which several strong interactions link all the components one by one and likely play a major role in AETFC assembly, while some weak interactions may further stabilize the complex.

To assess potentially joint functions of the AETFC components, we performed a ChIP-seq analysis of AML1-ETO, HEB, E2A and LMO2 in Kasumi-1 cells and validated some binding events by ChIP-qPCR – for example, on the well-established *CSF1R FIRE*²² and *SPI1 URE*²³ enhancers. Comparison of their binding sites and enrichment scores indicated a genome-wide colocalization and a correlation of binding strengths, and suggested that the interactions among the components facilitate their binding to the genome (Fig. 1d and Supplementary Fig. 4a–d). Sequence analysis of AML1-ETO-binding regions revealed that both AML1 sites and E-boxes (recognized by E proteins and other bHLH transcription factors including LYL1) were over-represented (Supplementary Fig. 4e, f), suggesting that, in addition to direct binding to DNA through the RUNT domain, AML1-ETO also binds to DNA indirectly through its interaction with the E-box-binding AETFC components.

To investigate the role of AETFC in regulating gene expression and leukaemogenesis, we performed gene knockdown in Kasumi-1 cells and in a mouse leukaemic model induced by AML1-ETO9a (AE9a), a leukaemogenic, truncated form of AML1-ETO²⁴. First of all, individual knockdowns of AETFC components (but not SCL) significantly decreased some other components at the protein level but not at the mRNA level (Supplementary Fig. 5a, b), suggesting a mutual stabilization mechanism within AETFC. Interestingly, *SCL* mRNA was downregulated by knockdown of any AETFC component (Supplementary Fig. 5b). Since the 3' haematopoietic enhancer of *SCL*²⁵ is bound by AETFC (Supplementary Fig. 5c), *SCL* is likely a direct target gene of AETFC. In an extension of this observation, global ChIP-seq and RNA-seq analyses revealed that the genes up- and down-regulated by one AETFC component were similarly regulated by others (Fig. 1e and Supplementary Fig. 5d). These analyses led to the identification of a set of genes that are both directly bound and cooperatively regulated by AETFC components (Supplementary Fig. 5e and Supplementary Tables 1, 2). We next showed that knockdowns of AETFC components considerably delayed leukaemogenesis in mice (Fig. 1f and Supplementary Fig. 6), indicating a requirement for AETFC components in AML1-ETO-mediated leukaemogenesis. Notably, double-knockdown of HEB and E2A most dramatically delayed leukaemogenesis, which is consistent with the primary importance of these two E proteins in AETFC assembly/stabilization (Fig. 1c and Supplementary Fig. 5a).

To further investigate the function and mechanism of these two E proteins in AETFC, we performed co-immunoprecipitation (co-IP) experiments with a series of deletion mutants of AML1-ETO and HEB, as well as a GST pull-down assay with isolated domains. These analyses clearly established multivalent interactions between AML1-ETO and E proteins and, interestingly, showed that the functionally critical NHR2 domain mediates not only oligomerization but also an interaction with E proteins (Supplementary Fig. 7). We next took several steps to clarify the relationship between NHR2-oligomerization and the NHR2-E protein interaction. First, we found that the multisite NHR2 mutation m7, which disrupts

NHR2-oligomerization⁴, also completely disrupts the NHR2-E protein interaction (Fig. 2a, b). Second, we performed an exhaustive screening of NHR2 mutations and found that NHR2-oligomerization and the NHR2-E protein interaction involve different surfaces of the NHR2 α -helix (Fig. 2a–d). Accordingly, we identified point mutations that specifically disrupt the NHR2-E protein interaction (Fig. 2b) but not NHR2-oligomerization, as indicated by co-IP (Supplementary Fig. 8) and gel-filtration (Fig. 2c) assays. Third, we found that the mutant-WT AML1-ETO heterodimer, unlike the WT homodimer, failed to bind HEB-AD1 (Fig. 2e), indicating that a single WT AML1-ETO in the dimer is unable to bind HEB-AD1 and, thus, that NHR2-oligomerization is required for the NHR2-E protein interaction.

To further clarify the mechanism of how E proteins recognize the NHR2 oligomer, we first mapped the NHR2-binding (N2B) region in HEB. As a result, we identified a novel, 18-amino acid N2B motif that is required for the NHR2-interaction (Fig. 3a, b, and Supplementary Fig. 9). A subsequent X-ray crystallographic analysis of the NHR2-N2B complex showed that NHR2 formed a tetrameric α -helical bundle⁴ with four N2B peptides bound on two symmetrically-related surfaces with 1:1 stoichiometry (Fig. 3c and Supplementary Fig. 10a). After an independent validation of directionality and register of the bound N2B peptide (Supplementary Fig. 10b, c), we demonstrated that a given N2B binds to a narrow surface channel created by two NHR2 helices, with P191 and S192 of N2B inserted deeply into a surface pocket (Fig. 3d). Notably, P191 of N2B interacts through hydrogen bonding with S522 from one NHR2 helix, while S192 and V194 form hydrogen bonds with E501 and H504, respectively, from another NHR2 helix (Fig. 3e). This unique interaction pattern confirms the results of the cell-based assay (Fig. 2e) by showing, unequivocally, that two dimerized NHR2 helices are required for the N2B-interaction. To further verify the binding specificity, we made mutations in NHR2 and in a shorter N2B(182-196) peptide and determined their interactions using fluorescence polarization (FP) assays. The results showed that the binding of such a short N2B peptide to NHR2 is relatively weak but highly specific since the mutation in NHR2 (mNHR2; Supplementary Fig. 11a) completely abolished the binding (Fig. 3f). Reciprocally, single mutations of the key residues P187, P191 or S192 of N2B also significantly reduced the binding, whereas mutation of the less important P188 had very little effect (Fig. 3g).

To study the biological relevance of the AML1-ETO–E protein interactions in leukaemogenesis, we introduced the mNHR2 mutation that specifically disrupts the NHR2-N2B interaction without affecting NHR2-oligomerization (Figs. 2c, 3f and Supplementary Fig. 11a, b), as well as the mNHR1 mutation that blocks the NHR1-AD1 interaction²⁶. We first employed the human CD34⁺ haematopoietic stem/progenitor cell (HSPC) self-renewal assay²⁷. While AML1-ETO and mutants exhibited comparable expression levels in transduced CD34⁺ cells (Supplementary Fig. 11c), mNHR2 significantly impaired the ability of AML1-ETO to maintain CD34⁺ cells (Fig. 4a). We also measured the frequencies of functional HSPCs using cobblestone area-forming cell (CAFC) and long-term culture-initiating cell (LTC-IC) assays. Notably, mNHR2 significantly reduced the CAFC and LTC-IC colonies in both assays, whereas mNHR1 showed relatively mild effects and no clear synergy between mNHR1 and mNHR2 was evident (Fig. 4b, c). These results suggest that the NHR2-N2B interaction, rather than simply acting additively with the NHR1-AD1

interaction to increase binding affinity, may act as a conformational switch within AETFC (Supplementary Fig. 1a) and thus contribute to AML1-ETO-enhanced HSPC self-renewal. In contrast, these mutations showed no effect on AML1-ETO activities in differentiation inhibition (Supplementary Fig. 12) and cell growth arrest (data not shown). To exclude the possibility that mNHR2 may affect other interactions rather than the E protein-interaction, we designed (based on the structure) another NHR2 mutation (mNHR2S) that effected a similar loss of E protein-binding but differed completely in sequence from mNHR2. Nevertheless, mNHR2 and mNHR2S showed similar effects in HSPC self-renewal and differentiation (Supplementary Fig. 13), strongly suggesting that these effects were specifically caused by disruption of the NHR2-N2B interaction.

To determine whether these interactions are also required for leukaemogenesis *in vivo*, we used the mouse leukaemic model²⁴ involving transplantation of mouse HSPCs transduced with WT and mutated AE9a. In this assay, mice carrying AE9a-mNHR2 showed a significant delay in leukaemogenesis compared with AE9a mice. First, AE9a-mNHR2 mice showed a significantly lower white blood cell (WBC) count than AE9a mice (Fig. 4d), consistent with peripheral blood morphology (Supplementary Fig. 14a). Second, mNHR2 mice had a lower percentage of c-Kit⁺/Mac-1⁻/GFP⁺ leukaemic blast cells in their peripheral blood (Supplementary Fig. 14b, c). Third, undifferentiated leukaemic cells were enriched in AE9a mice but not in mNHR2 mice (Fig. 4e). Finally, mNHR2 mice survived significantly longer than AE9a mice (Fig. 4f). The mNHR1 mutation again showed relatively mild effects in suppressing leukaemogenesis in mice. Taken together, both human HSPC and mouse transplantation assays clearly showed that the NHR2-N2B interaction is required for AML1-ETO-mediated leukaemogenesis. Given that the extremely high stability of the NHR2 oligomer makes its therapeutic targeting very challenging⁴, the NHR2-N2B interaction potentially offers a new target.

In contrast to previously reported dynamic interactions of various proteins with AML1-ETO under overexpression conditions, this study provides a direct and unbiased analysis of natural AML1-ETO in leukaemic cells and identification of an endogenous stable complex (AETFC). The multiple components in AETFC offer opportunities for recruitment of AML1-ETO to a variety of target genes and for regulation of gene expression through context-dependent functional interactions with diverse transcriptional coactivators and corepressors (Supplementary Figs. 1 and 15; further discussion in Supplementary Information). In leukaemic cells, most, if not all, AML1-ETO likely resides in and functions through AETFC since (i) knockdown of other AETFC components destabilizes AML1-ETO, (ii) many AML1-ETO-regulated genes are likewise co-occupied and co-regulated by AETFC components, and (iii) knockdowns of AETFC components significantly impair leukaemogenesis. Consistent with the observation that HEB and E2A play essential roles in AETFC assembly/stabilization and in leukaemogenesis, the direct AML1-ETO-E protein interaction is shown to be required for leukaemogenesis. Among the two defined AML1-ETO-E protein interaction sites, and surprisingly, the herein-identified and structurally characterized NHR2-N2B interaction, which requires oligomerization of NHR2, is necessary and sufficient for AML1-ETO-mediated leukaemogenesis (further discussed in Supplementary Information). Oligomerization of transcription factors has been known as an

important regulatory mechanism for modulating their DNA-binding specificity and affinity; and choice of different oligomerizing partners also contributes to selective recruitment of cofactors^{28,29}. Here, the unique NHR2-N2B interaction provides a novel model in which oligomeric transcription factors use their oligomerization domains to create a new protein-binding interface. Thus, this study reveals new mechanisms of action of the oligomerized AML1-ETO in leukaemogenesis and provides potential therapeutic possibilities.

Methods

Protein purification and mass spectrometry

Kasumi-1 cells were grown in 12 liter spinner flasks (BellCo) and the nuclear extract was prepared by our standard high salt extraction method³¹. The custom anti-ETO antibody (Covance) was developed against a C-terminal peptide of ETO and purified with a recombinant protein. Complex purification was performed in buffer BC300 (20 mM Tris, pH 7.3, 300 mM KCl, 0.2 mM EDTA and 20% Glycerol) plus 0.1% NP-40. Eluted proteins were separated by SDS-PAGE and visible bands on the gel were sliced separately and subjected to LC-MS/MS analysis. For immunoblot, the following antibodies were used: ETO (Santa Cruz; sc-9737), HEB (Santa Cruz; sc-357), E2A (Santa Cruz; sc-763), LDB1 (Santa Cruz; sc-11198), LYL1 (Abcam; ab30334), CBF β (Pierce; PA1-317), LMO2 (Abcam; ab81988) and SCL (a gift from Dr. R. Baer).

Gel filtration

The antigen-eluted complex was subjected to gel filtration with a Precision Column PC 3.2/30 that was pre-packed with Superose 6 and connected to an AKTA FPLC system (GE Healthcare). A Superdex 75 column (GE Healthcare) was used to determine the oligomeric states of WT and mutant AML1-ETO NHR2.

Reconstitution of protein complex

The Bac-to-Bac Baculovirus Expression Systems (Invitrogen) was used to generate recombinant baculoviruses containing each AETFC component. Reconstituted protein complexes were purified from Sf9 insect cells co-infected with different baculoviruses.

ChIP and ChIP-seq

Antigen-purified anti-ETO antibody and antibodies against HEB (Santa Cruz; sc-357), E2A (Santa Cruz; sc-763) and LMO2 (Abcam; ab81988) were used for ChIP and ChIP-seq assays. ChIP was performed with a dual cross-linking method. ChIP-seq libraries were constructed following the Illumina protocol and sequenced on the Illumina Genome Analyzer II. Peak-calling/annotation and consensus sequence analyses were performed with ChIPseeqer³², CisFinder³³ and Cisgenome³⁴.

shRNA knockdown

The shRNA against AML1-ETO was designed to target the fusion site. Other lentiviral shRNA sets were purchased from Open Biosystems. Virus preparation and cell infection

were performed according to manufacturer's protocol. Knockdown efficiencies were analyzed by RT-qPCR and/or immunoblot at 4 day post-infection.

RNA-seq

Kasumi-1 cells with knockdowns of AETFC components were harvested at 4 day post-infection and RNA was extracted with TRIzol Reagent (Invitrogen). Libraries were generated using the TruSeq RNA Sample Preparation Kit (Illumina) and sequenced with Illumina HiSeq2000. The reads were aligned with TopHat and then processed with an in-house program to calculate the RPKM value for each gene following published methods³⁵.

Cell transfection and co-immunoprecipitation

293T cells were transfected using Lipofactamine 2000 (Invitrogen). Cells lysis and Co-IP were performed with T/G lysis buffer (20 mM Tris-HCl, pH 7.5, 300 mM NaCl, 50 mM NaF, 2 mM EDTA, 1% Triton X-100 and 20% Glycerol), and proteins were analyzed by immunoblot.

GST pull-down

GST-tagged proteins were expressed in *E. coli* and purified with glutathione Sepharose 4B (GE Healthcare). The ³⁵S-labelled prey proteins were synthesized with the TNT Quick Coupled Transcription/Translation System (Promega). Pull-down assays were performed with NETN buffer (20 mM Tris-HCl, pH 8.0, 100 mM NaCl, 1 mM EDTA and 0.5% NP-40), followed by SDS-PAGE and autoradiography analyses.

Co-expression of N2B fragment and NHR2 domain

The His-Sumo-tagged N2B(100-219) fragment of HEB and the GST-tagged NHR2(482-551) domain of AML1-ETO were co-expressed in *E. coli* and purified by GST- or His-pull down. By serial truncation of N2B from both ends, a short N2B(177-200) peptide was shown to retain its binding affinity for NHR2, and this N2B fragment was used for crystallization trials.

Crystallization and structure determination

Purified N2B(177-200) peptide and NHR2(486-548) domain were mixed at around 1:1 ratio and subjected to crystallization trials. Crystals of the complex were grown by the hanging-drop method at 20°C in buffer containing 0.1 mM Tris (pH 8.5) and 20% ethanol. A 2.9 Å resolution data set of the complex was collected on beamline 24ID-E at the Advanced Photon Source, Argonne National Laboratory. The initial model was solved by molecular replacement using the free NHR2 structure as the search model. The validation of the directionality and register of the bound N2B peptide were performed with the selenomethionine labeling method following the introduction of V186M, V194M and corresponding double mutations.

Fluorescence polarization-based measurements

Peptides were labeled with fluorescein at the N-terminus. FP assays were carried out and analyzed using FP buffer (10 mM TEA, 20 mM NaCl, pH 7.4)³⁶. Titration series of protein

in 10 μ l volume and containing 100 nM fluorescinated peptide in 384-well plates were read multiple times on a Plate Chameleon II plate reader (HIDEX Oy).

Human HSPC self-renewal and differentiation

CD34⁺ cells were purified from human cord blood samples using the MACS CD34 Isolation Kit (Miltenyi Biotec). After expansion, cells were infected with MIGR1-derived retroviruses. GFP⁺/CD34⁺ cells were sorted and grown in basic or differentiation medium and re-plated weekly. Numbers of HSPC and differentiated cells were determined by cell counting and flow cytometry. For the CAFC assays, CD34⁺ cells were co-cultured on an MS-5 monolayer and demi-depopulated weekly. The cobblestone areas were scored at week 5. For LTC-IC assays, the cells were plated at week 6 in methylcellulose with cytokines, and the colony numbers were scored 14 days after seeding.

Mouse fetal liver transplantation and leukaemogenesis assays

Mouse fetal liver HSPCs were infected with MIGR1-derived retroviruses and cultured in X-VIVO medium (Lonza) with cytokines. Recipient mice were lethally irradiated and transduced fetal liver cells were transplanted into recipient mice by tail-vein injection. Leukaemia development was determined by complete blood count, flow cytometry and morphological analyses of peripheral blood and bone marrow cells. The overall survival of the mice was analyzed by Kaplan-Meier method and the statistical significance was evaluated by the logrank test. For bioluminescent imaging of leukaemia in mice³⁷, AE9a leukaemic cells were transduced with MSCV-Luciferase PGK-hygo (Addgene). Upon injection of the substrate of luciferase, D-Luciferin, bioluminescent imaging was performed using an IVIS100 imaging system. For gene knockdown assays in the mouse model, a mouse leukaemic cell line was generated from the spleen of the mice bearing AE9a-induced leukaemia. These cells were infected with shRNA lentiviruses, selected by puromycin and injected into recipient mice to generate leukaemia.

Supplementary Material

Refer to Web version on PubMed Central for supplementary material.

Acknowledgments

We thank N. A. Speck and J. H. Bushweller for providing AML1-ETO m7 plasmid, and R. Baer for providing SCL plasmids and anti-SCL antibodies. This work was supported by National Institutes of Health (NIH) grants CA163086 (R.G.R.), CA129325 (R.G.R.), CA113872 (R.G.R.) and CA166835 (S.D.N.), Starr Cancer Consortium grant I5-A554 (R.G.R., D.J.P. and S.D.N.), Leukemia and Lymphoma Society (LLS) SCOR grants 7013-02 (R.G.R. and S.D.N.) and 7132-08 (R.G.R., A.M. and D.J.P.), and Rockefeller University Center for Clinical and Translational Science Pilot Project grant UL1RR024143 from NIH (X.-J.S.). X.J.S. was a Starr Cancer Consortium Visiting Fellow. L.W. was an Empire State Stem Cell Scholar and an LLS Fellow. W.Y.C. was an LLS Fellow. D.J.P. was supported by funds from Abby Rockefeller Mauze Trust and the Maloris Foundation.

References

1. Look AT. Oncogenic transcription factors in the human acute leukemias. *Science*. 1997; 278:1059–1064. [PubMed: 9353180]
2. Peterson LF, Zhang DE. The 8;21 translocation in leukemogenesis. *Oncogene*. 2004; 23:4255–4262. [PubMed: 15156181]

3. Minucci S, et al. Oligomerization of RAR and AML1 transcription factors as a novel mechanism of oncogenic activation. *Mol Cell*. 2000; 5:811–820. [PubMed: 10882117]
4. Liu Y, et al. The tetramer structure of the Nervy homology two domain, NHR2, is critical for AML1/ETO's activity. *Cancer Cell*. 2006; 9:249–260. [PubMed: 16616331]
5. Kwok C, Zeisig BB, Qiu J, Dong S, So CW. Transforming activity of AML1-ETO is independent of CBFbeta and ETO interaction but requires formation of homo-oligomeric complexes. *Proc Natl Acad Sci U S A*. 2009; 106:2853–2858. [PubMed: 19202074]
6. Yan M, Ahn EY, Hiebert SW, Zhang DE. RUNX1/AML1 DNA-binding domain and ETO/MTG8 NHR2-dimerization domain are critical to AML1-ETO9a leukemogenesis. *Blood*. 2009; 113:883–886. [PubMed: 19036704]
7. Okumura AJ, Peterson LF, Okumura F, Boyapati A, Zhang DE. t(8;21)(q22; q22) Fusion proteins preferentially bind to duplicated AML1/RUNX1 DNA-binding sequences to differentially regulate gene expression. *Blood*. 2008; 112:1392–1401. [PubMed: 18511808]
8. Gelmetti V, et al. Aberrant recruitment of the nuclear receptor corepressor-histone deacetylase complex by the acute myeloid leukemia fusion partner ETO. *Mol Cell Biol*. 1998; 18:7185–7191. [PubMed: 9819405]
9. Lutterbach B, et al. ETO, a target of t(8;21) in acute leukemia, interacts with the N-CoR and mSin3 corepressors. *Mol Cell Biol*. 1998; 18:7176–7184. [PubMed: 9819404]
10. Wang J, Hoshino T, Redner RL, Kajigaya S, Liu JM. ETO, fusion partner in t(8;21) acute myeloid leukemia, represses transcription by interaction with the human N-CoR/mSin3/HDAC1 complex. *Proc Natl Acad Sci U S A*. 1998; 95:10860–10865. [PubMed: 9724795]
11. Westendorf JJ, et al. The t(8;21) fusion product, AML-1-ETO, associates with C/EBP-alpha, inhibits C/EBP-alpha-dependent transcription, and blocks granulocytic differentiation. *Mol Cell Biol*. 1998; 18:322–333. [PubMed: 9418879]
12. Mao S, Frank RC, Zhang J, Miyazaki Y, Nimer SD. Functional and physical interactions between AML1 proteins and an ETS protein, MEF: implications for the pathogenesis of t(8;21)-positive leukemias. *Mol Cell Biol*. 1999; 19:3635–3644. [PubMed: 10207087]
13. Elagib KE, et al. RUNX1 and GATA-1 coexpression and cooperation in megakaryocytic differentiation. *Blood*. 2003; 101:4333–4341. [PubMed: 12576332]
14. Zhang J, Kalkum M, Yamamura S, Chait BT, Roeder RG. E protein silencing by the leukemogenic AML1-ETO fusion protein. *Science*. 2004; 305:1286–1289. [PubMed: 15333839]
15. Gardini A, et al. AML1/ETO oncoprotein is directed to AML1 binding regions and co-localizes with AML1 and HEB on its targets. *PLoS Genet*. 2008; 4:e1000275. [PubMed: 19043539]
16. Guo C, Hu Q, Yan C, Zhang J. Multivalent binding of the ETO corepressor to E proteins facilitates dual repression controls targeting chromatin and the basal transcription machinery. *Mol Cell Biol*. 2009; 29:2644–2657. [PubMed: 19289505]
17. Martens JH, et al. ERG and FLI1 binding sites demarcate targets for aberrant epigenetic regulation by AML1-ETO in acute myeloid leukemia. *Blood*. 2012; 120:4038–4048. [PubMed: 22983443]
18. Wang L, et al. The leukemogenicity of AML1-ETO is dependent on site-specific lysine acetylation. *Science*. 2011; 333:765–769. [PubMed: 21764752]
19. Shia WJ, et al. PRMT1 interacts with AML1-ETO to promote its transcriptional activation and progenitor cell proliferative potential. *Blood*. 2012; 119:4953–4962. [PubMed: 22498736]
20. Miyoshi H, et al. The t(8;21) translocation in acute myeloid leukemia results in production of an AML1-MTG8 fusion transcript. *EMBO J*. 1993; 12:2715–2721. [PubMed: 8334990]
21. Wadman IA, et al. The LIM-only protein Lmo2 is a bridging molecule assembling an erythroid, DNA-binding complex which includes the TAL1, E47, GATA-1 and Ldb1/NLI proteins. *EMBO J*. 1997; 16:3145–3157. [PubMed: 9214632]
22. Follows GA, et al. Epigenetic consequences of AML1-ETO action at the human c-FMS locus. *EMBO J*. 2003; 22:2798–2809. [PubMed: 12773394]
23. Huang G, et al. PU.1 is a major downstream target of AML1 (RUNX1) in adult mouse hematopoiesis. *Nat Genet*. 2008; 40:51–60. [PubMed: 17994017]
24. Yan M, et al. A previously unidentified alternatively spliced isoform of t(8;21) transcript promotes leukemogenesis. *Nat Med*. 2006; 12:945–949. [PubMed: 16892037]

25. Sanchez M, et al. An SCL 3' enhancer targets developing endothelium together with embryonic and adult haematopoietic progenitors. *Development*. 1999; 126:3891–3904. [PubMed: 10433917]
26. Park S, et al. Structure of the AML1-ETO eTAFH domain-HEB peptide complex and its contribution to AML1-ETO activity. *Blood*. 2009; 113:3558–3567. [PubMed: 19204326]
27. Mulloy JC, et al. The AML1-ETO fusion protein promotes the expansion of human hematopoietic stem cells. *Blood*. 2002; 99:15–23. [PubMed: 11756147]
28. Amoutzias GD, Robertson DL, Van de PY, Oliver SG. Choose your partners: dimerization in eukaryotic transcription factors. *Trends Biochem Sci*. 2008; 33:220–229. [PubMed: 18406148]
29. Funnell AP, Crossley M. Homo- and heterodimerization in transcriptional regulation. *Adv Exp Med Biol*. 2012; 747:105–121. [PubMed: 22949114]
30. Heidenreich O, et al. AML1/MTG8 oncogene suppression by small interfering RNAs supports myeloid differentiation of t(8;21)-positive leukemic cells. *Blood*. 2003; 101:3157–3163. [PubMed: 12480707]
31. Dignam JD, Lebovitz RM, Roeder RG. Accurate transcription initiation by RNA polymerase II in a soluble extract from isolated mammalian nuclei. *Nucleic Acids Res*. 1983; 11:1475–1489. [PubMed: 6828386]
32. Giannopoulou EG, Elemento O. An integrated ChIP-seq analysis platform with customizable workflows. *BMC Bioinformatics*. 2011; 12:277. [PubMed: 21736739]
33. Sharov AA, Ko MS. Exhaustive search for over-represented DNA sequence motifs with CisFinder. *DNA Res*. 2009; 16:261–273. [PubMed: 19740934]
34. Ji H, et al. An integrated software system for analyzing ChIP-chip and ChIP-seq data. *Nat Biotechnol*. 2008; 26:1293–1300. [PubMed: 18978777]
35. Mortazavi A, Williams BA, McCue K, Schaeffer L, Wold B. Mapping and quantifying mammalian transcriptomes by RNA-Seq. *Nat Methods*. 2008; 5:621–628. [PubMed: 18516045]
36. Jacobs SA, Fischle W, Khorasanizadeh S. Assays for the determination of structure and dynamics of the interaction of the chromodomain with histone peptides. *Methods Enzymol*. 2004; 376:131–148. [PubMed: 14975303]
37. Zuber J, et al. Mouse models of human AML accurately predict chemotherapy response. *Genes Dev*. 2009; 23:877–889. [PubMed: 19339691]

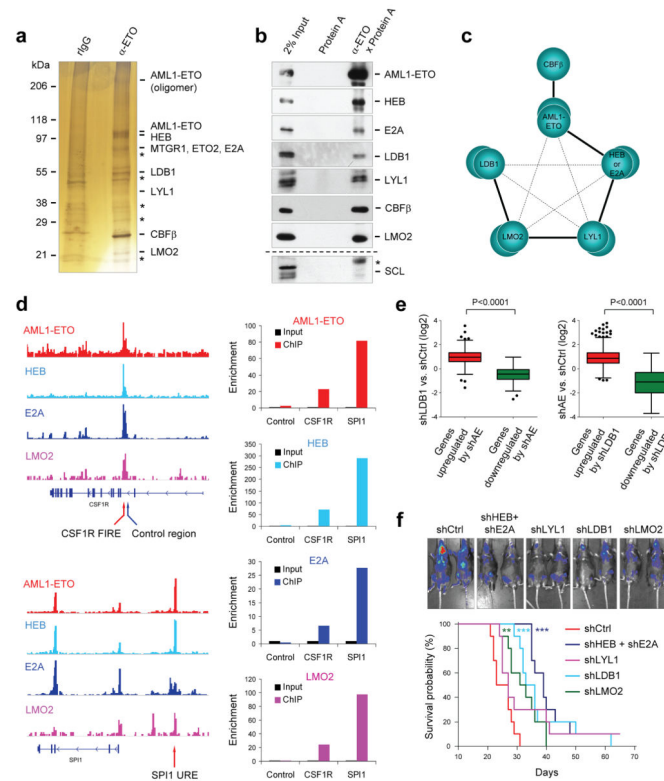


Figure 1. AML1-ETO resides in and functions through AETFC

a, SDS-PAGE and silver staining of AETFC isolated from Kasumi-1 nuclear extract. Asterisks, non-specific bands. **b**, Co-IP and immunoblot confirmation of AETFC components. Asterisk, IgG signal. **c**, Schematic of interactions within AETFC. Thick and thin lines denote strong and weak interactions, respectively. Double spheres denote potential homodimerization of components. **d**, CHIP-seq and ChIP-qPCR analyses of AETFC components on *CSF1R* and *SPI1*. **e**, Correlation between AE and LDB1 in regulating gene expression. **f**, Knockdown of AETFC components delays AE9a-induced leukaemogenesis in mice, indicated by representative bioluminescent imaging (upper) and survival curves (bottom; $n = 10$; $***P < 0.001$; $**P < 0.01$).

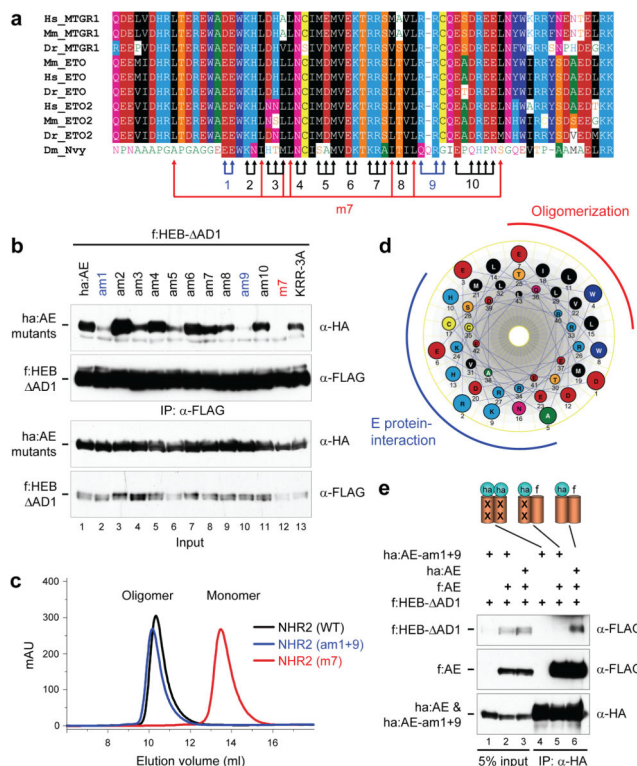


Figure 2. Oligomerized AML1-ETO NHR2 domain mediates a specific interaction with E proteins

a, Alignment of NHR2 of ETO family proteins. Arrows denote residues mutated to alanine in mutants am1–10 screened herein and the m7 mutant that disrupts NHR2-oligomerization⁴. **b**, Identification of mutations that disrupt the interaction between AE and HEB- AD1. **c**, Gel-filtration profiles of WT and mutant NHR2. WT and am1+9 were eluted as oligomers, and m7 as a monomer. **d**, Distinct surfaces of the NHR2 α -helix mediate oligomerization and the E protein interaction. **e**, NHR2-oligomerization is required for the NHR2-E protein interaction. Mutant-mutant AE homodimer (lanes 1, 4), mutant-WT heterodimer (lanes 2, 5) and WT-WT homodimer (lanes 3, 6) were formed in 293T cells by co-expression of WT AE and NHR2-mutated AE (“XX”) that fails to interact with HEB-AD1, and their abilities to bind to HEB- AD1 were determined by co-IP.

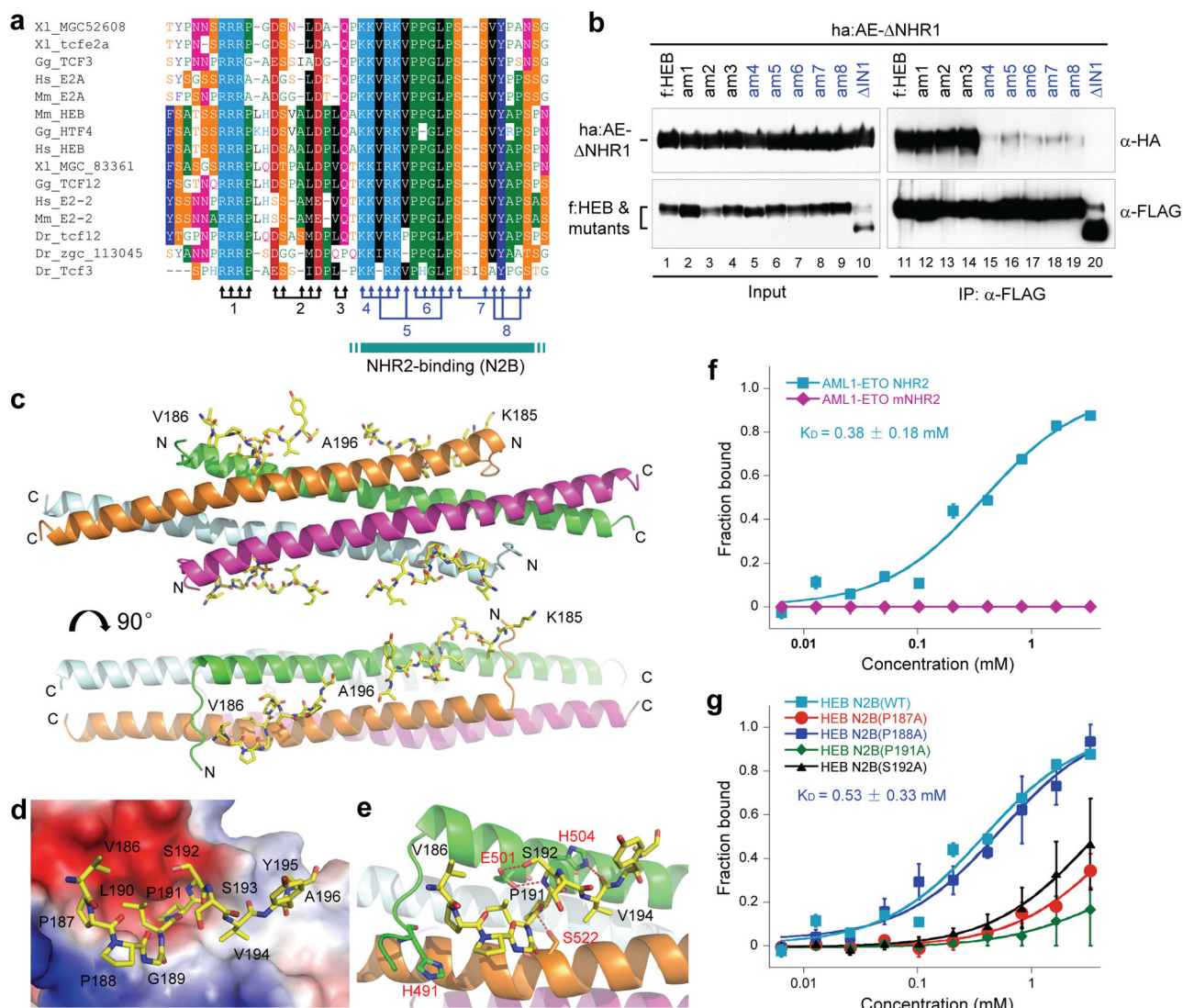


Figure 3. Structural details of the NHR2-N2B interaction

a, Alignment of the N2B regions of vertebrate E proteins. Arrows denote residues mutated to alanine in mutants am1–8. **b**, Identification of the N2B motif by co-IP. **c**, Side (upper) and look-down (bottom) ribbon views of the structure of the complex between the N2B(177-200) peptide and the tetrameric-helical bundle of NHR2. The N2B peptide is shown in stick representation, and the NHR2 helices in ribbon representation. **d**, Positioning of the N2B peptide on the electrostatic surface of the NHR2 tetramer. **e**, One N2B peptide interacts with two NHR2 helices through hydrogen bonds. **f**, **g**, FP analysis of the binding between NHR2 and a shorter N2B(182-196) peptide, comparing WT and indicated mutants of NHR2 (**f**) and N2B (**g**). $n=3$; mean \pm s.d.

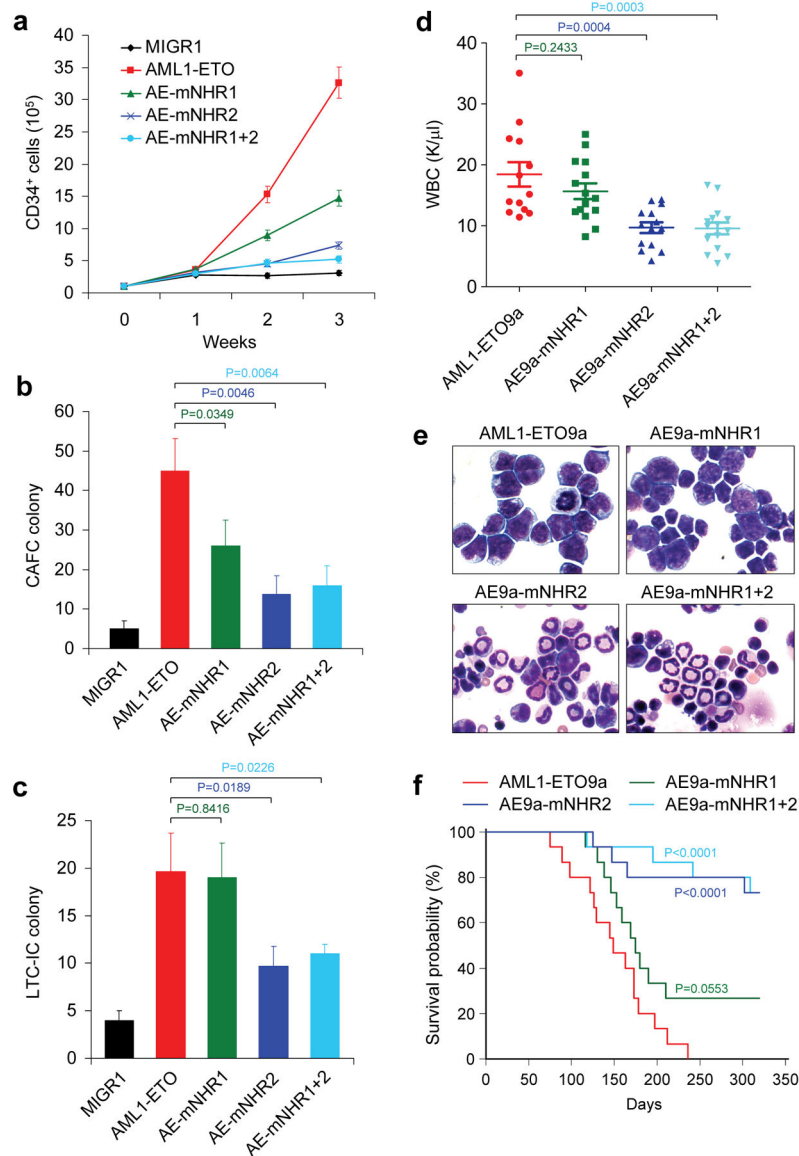


Figure 4. Role of the AML1-ETO-E protein interactions in human HSPC self-renewal and mouse leukaemogenesis

a, Effects of AE and derived mutants in maintenance of human CD34⁺ cells. **b**, CAFC assays measuring the frequency of functional HSPCs in cells transduced with AE or derived mutants. **c**, LTC-IC assays measuring the frequency of functional HSPCs after long-term *in vitro* culture of cells transduced with AE or derived mutants. In **a–c**, $n=3$; mean \pm s.d. **d**, Effects of AE9a and derived mutants in mouse leukaemogenesis, as indicated by WBC count of peripheral blood at 4 months post transplantation. **e**, Morphological analysis of mouse bone marrow cells. **f**, Kaplan-Meier survival curves of the mice ($n = 15$).